J. At. Mol. Sci.
doi: 10.4208/jams.040815.050415a

Vol. **6**, No. 2, pp. 119-128
June 2015

Molecular orientation effect on the photodetachment of a diatomic molecular anion

Zhao-Ming Zhong and De-Hua Wang*

School of Physics and Optoelectronic Engineering, Ludong University, Yantai 264025, China

Received 8 April 2015; Accepted (in revised version) 4 May 2015
Published Online 6 June 2015

Abstract. The interference effect in the photdetachment of a diatomic molecular anion is investigated theoretically for different molecular orientation by using the two-center model. An analytic formula is presented for the photodetached electron flux distribution at a given observation plane. Taking H_2^- as an example, we calculate the electron flux distribution and photodetachment cross section for arbitrary molecular orientation. The results show that the molecular orientation has great influence on the photodetachment of the diatomic molecular anion. At certain molecular orientation, the interference in the electron flux distribution is totally constructive; while at some other orientations, the interference is destructive. For molecular orientation along the laser light polarization, the oscillation amplitude in the photodetachment cross section is the largest; however, for the molecular orientation perpendicular to the laser light polarization, no oscillation appears in the cross section. Our studies suggest that we can control the photodetachment process of the molecular negative ion by changing the molecular orientation. Our researches will be helpful for the theoretical and experimental study of the photodetachment of molecular anion.

PACS: 32.80.Fb, 33.80.Eh,34.80.Gs

Key words: molecular orientation, photodetachment, interference, two-center model.

1 Introduction

During the past two decades, many researchers have studied the photodetachment of negative ion in various external fields [1-12]. As a simple one-center model system, the photodetachment of H^- ion have been investigated both theoretically and experimentally. It has been found that the photodetachment cross sections of H^- in external fields display oscillatory structures. Since the photodetachment cross section is proportional to

*Corresponding author. *Email address:* lduwdh@163.com (D.-H. Wang)

the integrated outgoing electron flux across a large enclosure in which the bound H^- sits, therefore it is clear that the oscillation in the total cross section of H^- in external fields reflects the interferences in the spatial distribution of the electron flux. Recently, with the development of the molecular photodetachment microscopy, the photodetachment of negative molecular ion has attracted a lot of attention [13-15]. Since 2006, Afraq and Du have studied the photodetachment of a negative hydrogen molecular ion in the absence of external fields by using a two-centre model and discussed the interference effect of the nuclei [16-17]. In their works, they studied in great detail the dependence of the cross section on the distance between the two nuclei, photon energy and the laser polarization. Their results suggest when the molecular axis of the diatomic molecular anion is perpendicular to the laser polarization, the total photodetachment cross section is still smooth curve; while for the molecular orientation is parallel to the laser polarization, oscillation appears in the cross section. Based upon their work, we discussed the photodetachment of a diatomic molecular anion with the molecular axis orientation varied in a fixed plane [18]. Then what will happen for arbitrary spatial molecular orientation? None has given the discussion.

In this paper, by using the two-center model, we study the photodetachment of a diatomic molecular anion with arbitrary spatial molecular orientation. The two atomic centers in the diatomic molecular anion are assumed to interact with one another to an extent sufficient to establish two coherent sources of detached electrons. When interacting with a laser, each center is assumed to produce an outgoing wave similar to that in H^-. These outgoing waves propagate to large distances. Sufficiently far from the molecular anion, the wave propagates according to semiclassical mechanics, and it is correlated with classical trajectories. Two classical trajectories for a photodetached electron propagating along two distant paths starting from each center to an observation point produce the interference pattern in the electron flux distribution on the screen. The detached-electron flux on the screen can be calculated analytically. By integrating the detached-electron flux for all outgoing directions, we are able to calculate the photodetachment cross section with arbitrary molecular orientation.

2 Theoretical method

The schematic diagram of the system is shown in Fig. 1. Suppose the diatomic molecular anion is placed in the x-y-z plane. The two circles represent the two centers of the negative molecular ion, d is the distance between the two centers. θ_D is the angle between the molecular axis and z-axis, and φ_D is the azimuth angle. The observation plane is placed perpendicular to z-axis and the laser light is polarized along the +z-direction.

As in Ref. [14], we assume that there is only one active electron in the molecular anion system and the active electron is loosely bound by a short-range, spherically symmetric molecular core potential $V_b(r)$, where r is the distance between the active electron and the origin of the system. Before photodetachment, the normalized wave

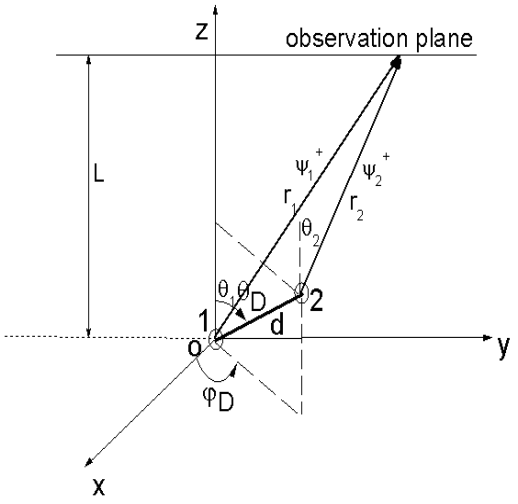

Figure 1: Schematic diagram for the photodetachment of diatomic molecular anion with arbitrary molecular orientation. The two circles represent the two centers of the molecular anion. The observation plane is placed at a distance L from the origin perpendicular to z-axis, d is the distance between the two centers. $(\theta_D,\ \varphi_D)$ is the molecular orientation. Two outgoing waves propagating away from each center are shown.

function for the active electron in molecular anion can be written as a linear combination of the detached electron's wave function of the negative ion at the two centers [19]: $\phi_M = \frac{1}{\sqrt{2}}(\phi_1+\phi_2)$.Where ϕ_1, ϕ_2 are the normalized initial wave function of the negative ion centered in the two nuclei, $\phi_1 = B\frac{e^{ik_b r_1}}{r_1}$ and $\phi_2 = B\frac{e^{ik_b r_2}}{r_2}$. r_1 and r_2 are the distances of the active electron relative to center 1 and center 2 respectively. B is a constant and k_b is related to the binding energy of the negative ion by $E_b = k_b^2/2$. After the molecular anion absorbs photon energies E_{ph}, outgoing electron waves are generated. The detached electron wave function is a superposition of detached waves generated from the two centers. Let ψ_1^+ and ψ_2^+ be the waves emitting from center 1 and 2 respectively, then the outgoing electron wave ψ_M^+ form the negative molecular ion is given by:

$$\psi_M^+ = \frac{1}{\sqrt{2}}(\psi_1^+ + \psi_2^+). \tag{1}$$

Using $(r_1,\ \theta_1,\ \phi_1)$ and $(r_2,\ \theta_2,\ \phi_2)$ as the spherical coordinates of the detached electron relative to each center, we have:

$$\psi_1^+(r_1,\ \theta_1,\ \phi_1) = U(k,\ \theta_1,\ \phi_1)\frac{e^{ikr_1}}{r_1}, \quad \psi_2^+(r_2,\ \theta_2,\ \phi_2) = U(k,\ \theta_2,\ \phi_2)\frac{e^{ikr_2}}{r_2}. \tag{2}$$

The factors $U(k,\ \theta_1,\ \phi_1)$ and $U(k,\ \theta_2,\ \phi_2)$ for the laser polarization parallel to z-axis can be written as

$$U(k,\ \theta_1,\ \phi_1) = C\cos\theta_1, \quad U(k,\ \theta_2,\ \phi_2) = C\cos\theta_2. \tag{3}$$

Where $C = \frac{4kBi}{(k_b^2+k^2)^2}$, $k = \sqrt{2E}$, with E is the energy of the detached electron.

Therefore the detached electron wave function from the negative molecular ion ψ_M^+ can be written as:

$$\psi_M^+(r,\theta,\phi)=\frac{C}{\sqrt{2}}[\cos\theta_1\frac{e^{ikr_1}}{r_1}+\cos\theta_2\frac{e^{ikr_2}}{r_2}]. \tag{4}$$

(r,θ,φ) is the spherical coordinates of the detached electron relative to the origin, then $r_1=r$, $\theta_1=\theta$, $\varphi_1=\varphi$. Because the distance between the observation plane and the negative molecular ion is much greater than the distance d between the two centers, the above formula (Eq. (4)) can be simplified further. In the phase terms, we use:

$$r_2\approx r-(d\sin\theta_D\cos\varphi_D)\sin\theta\cos\varphi-(d\sin\theta_D\sin\varphi_D)\sin\theta\sin\varphi-(d\cos\theta_D)\cos\theta. \tag{5}$$

And in all other places use $r_1\approx r_2\approx r$ and $\theta_1\approx\theta_2\approx\theta$.

With these approximations, Eq. (4) becomes

$$\begin{aligned}\psi_M^+(r,\theta,\phi)=\frac{C}{\sqrt{2}}\frac{e^{ikr}}{r}\cos\theta(1+\exp\{-ikd[&(\sin\theta_D\cos\varphi_D)\sin\theta\cos\varphi\\&+(\sin\theta_D\sin\varphi_D)\sin\theta\sin\varphi+(\cos\theta_D)\cos\theta]\}).\end{aligned} \tag{6}$$

For a given observation plane perpendicular to the z axis, the electron flux on that plane in the radial direction at large r is :

$$j_r(r,\theta,\varphi)=\frac{i}{2}(\psi_M^+)\frac{\partial\psi_M^{+^*}}{\partial r}-\psi_M^{+^*}\frac{\partial\psi_M^+}{\partial r}. \tag{7}$$

Substituting Eq. (6) into the above formula, we get:

$$\begin{aligned}j_r(r,\theta,\varphi)=\frac{k|C|^2\cos^2\theta}{r^2}(1+\cos\{kd[&(\sin\theta_D\cos\varphi_D)\sin\theta\cos\varphi\\&+(\sin\theta_D\sin\varphi_D)\sin\theta\sin\varphi+(\cos\theta_D)\cos\theta]\}).\end{aligned} \tag{8}$$

In order to obtain the flux on the observation plane, we project the flux in Eq. (8) in the normal direction of the plane:

$$j_z(r,\theta,\varphi)=j_r(r,\theta,\varphi)\hat{r}\cdot\hat{n}. \tag{9}$$

Since $\hat{r}\cdot\hat{n}=\cos\theta$, so we get

$$\begin{aligned}j_z(r,\theta,\varphi)=\frac{k|C|^2\cos^3\theta}{r^2}(1+\cos\{kd[&(\sin\theta_D\cos\varphi_D)\sin\theta\cos\varphi\\&+(\sin\theta_D\sin\varphi_D)\sin\theta\sin\varphi+(\cos\theta_D)\cos\theta]\}).\end{aligned} \tag{10}$$

From the above formula, we find that the electron flux distribution is related to the molecular orientation (θ_D,φ_D).

When the molecular axis orientation is parallel to z-axis, by setting θ_D in Eq. (10), we get:

$$j_z(r,\theta,\varphi)=\frac{k|C|^2\cos^3\theta}{r^2}\{1+\cos[kd(\cos\theta)]\}. \tag{11}$$

When the molecular axis orientation is perpendicular to z-axis, by setting $\theta_D=\pi/2$, $\varphi_D=\pi/2$ in Eq. (10), we get:

$$j_z(r,\theta,\varphi)=\frac{k|C|^2\cos^3\theta}{r^2}\{1+\cos[kd(\sin\theta\sin\phi)]\}. \tag{12}$$

The above two special cases are studied by Afaq and Du earlier for the photodetachment of H_2^- [16-17]. If we set $\varphi_D=\pi/2$ and change the value of θ_D, we find this situation likes the case of the molecular orientation in y-z plane [18].

Next, we calculate the total photodetachment cross section of the diatomic molecular anion with arbitrary molecular orientation. Imagine a large surface Γ such as the surface of a sphere enclosing the source region, the differential cross section on that surface is defined as:

$$\frac{d\sigma(q)}{ds}=\frac{2\pi E_{ph}}{c}\vec{j_r}\cdot\hat{n}. \tag{13}$$

Where c is the speed of light and $E_{ph}=E+E_b$ is the photon energy, q is the coordinate on the surface, $\hat{n}$ is exterior norm vector at q, $ds=r^2\sin\theta d\theta d\varphi$ is the differential area on the spherical surface. The total cross section can be obtained by integrating the differential cross section over the surface, $\sigma(E)=\int\frac{d\sigma(q)}{ds}ds$.

In the present case, we haveG

$$\begin{aligned}\sigma(E)=&\frac{2\pi k|C|^2E_{ph}}{c}\int_0^{2\pi}\int_0^{\pi}\cos^2\theta\sin\theta(1+\cos\{kd[\sin\theta_D\cos\varphi_D)\sin\theta\cos\varphi\\&+(\sin\theta_D\sin\varphi_D)\sin\theta\sin\varphi+(\cos\theta_D)\cos\theta]\})d\theta d\phi.\end{aligned} \tag{14}$$

From this formula, we find that the total cross section is related to the molecular orientation $(\theta_D,\ \varphi_D)$. When the molecular orientation is perpendicular to z-axis, by setting $\theta_D=\pi/2$, $\varphi_D=\pi/2$ and integrating Eq. (14) , we get:

$$\sigma(E)=\sigma_0(E)[1+\frac{3(-kd\cos(kd)+\sin(kd))}{(kd)^3}]. \tag{15}$$

For the parallel case, by setting $\theta_D=0$ and integrating Eq. (14) , we obtain:

$$\sigma(E)=\sigma_0(E)[1+\frac{3\sin(kd)}{(kd)}+\frac{6\cos(kd)}{(kd)^2}-\frac{6\sin(kd)}{(kd)^3}]. \tag{16}$$

The above two analytical formula are discussed by Afaq and Du for the total photodetachment cross section of H_2^- in Ref. [16-17].

As for the arbitrary molecule orientation, Eq. (14) cannot be integrated analytically, but once the molecular orientation (θ_D, φ_D) is given, we can still calculate the photodetachment cross section by using the numerical integration method easily. For the H_2^-, the constants B and k_b in the electron flux and cross section are as follows: B=0.31552, k_b=0.2345.

3 Results and discussions

Suppose the laser is polarized in the z direction, the distance between the observation plane and the origin is L, then the detached electron flux in the z-direction is:

$$j_z(r,\theta,\varphi)=\frac{k|C|^2L^3}{r^5}(1+\cos\{kd[(\sin\theta_D\cos\varphi_D)\frac{x}{r}+(\sin\theta_D\sin\varphi_D)\frac{y}{r}+(\cos\theta_D)\frac{L}{r}]\}). \quad (17)$$

Here $r=(x^2+y^2+L^2)^{1/2}$.

By using Eq. (17), we calculate the photodetachment electron flux distribution of H_2^- with different molecular orientation at a given observation plane on the x=0 line, the

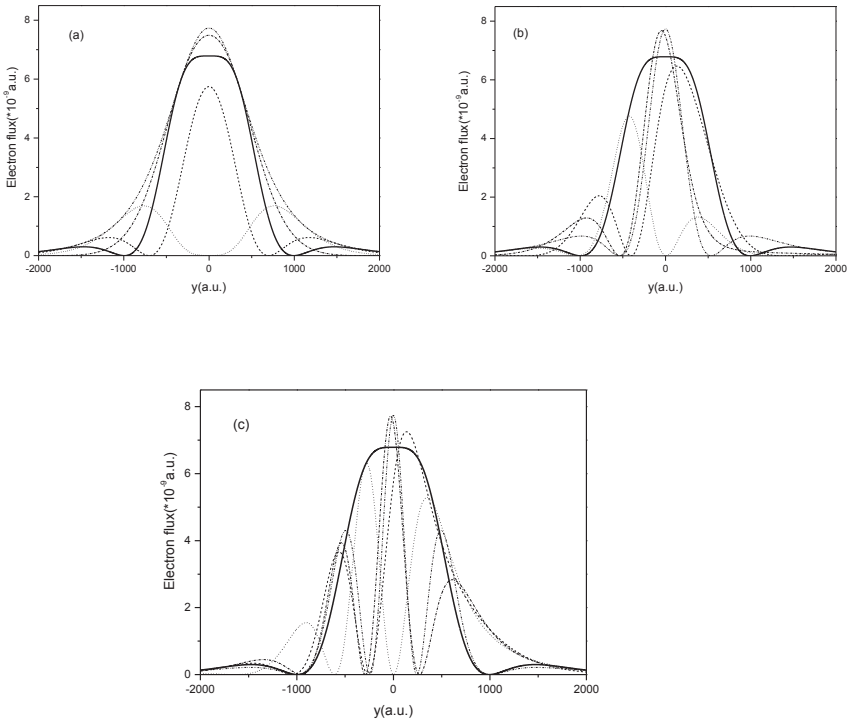

Figure 2: The variation of the electron flux distribution for the photodetachment of H_2^- with different φ_D. (a) $\varphi_D=0$, (b) $\varphi_D=\pi/6$, (c) $\varphi_D=\pi/2$. The solid line is $\theta_D=0$, the dashed line is $\theta_D=\pi/6$, the dotted line is $\theta_D=\pi/4$, the dash-dotted line is $\theta_D=\pi/3$ and the dash-dotted-dotted line is $\varphi_D=\pi/2$.

distance between the two centers of H_2^- is d=4.0a.u.. The photon energy $E_{ph}=150eV$ and the distance between the origin and the observation plane is L=1000a.u.. The results are given in Figs. 2-4. In each plot of Fig. 2, we fix the azimuth angle φ_D and change the value of θ_D. Fig. 2(a) is the case when $\varphi_D=0$ and θ_D is varied between 0 and $\pi/2$. Under this situation, the molecular axis lies in the x-z plane. From this plot we find, the electron flux distribution is symmetric about y-axis. As the angle between the molecular orientation and z axis is $\theta_D=\pi/2$, the oscillation amplitude is the largest. The oscillation amplitude is the smallest with $\theta_D=\pi/4$. For other angle θ_D, the oscillation amplitude is varied between the maximum and minimum. Fig. 2(b) is the case with $\varphi_D=\pi/6$ and θ_D is varied between 0 and $\pi/2$. This plot suggests that as $\theta_D=\pi/2$, the electron flux distribution is symmetric about y-axis, and its oscillation amplitude is the largest. With the decrease of θ_D, the oscillation amplitude becomes decreased. At $\theta_D=\pi/4$, the oscillation amplitude is the smallest. As we further increase θ_D, the oscillation amplitude increases again. Fig. 2(c) is the case with $\varphi_D=\pi/2$ and θ_D is changed from 0 to $\pi/2$. Under this condition, the molecule axis lies in the y-z plane. At $\theta_D=\pi/2$, the molecular orientation is along the y-axis and is perpendicular to the laser light polarized along z direction [16], the oscillation in the electron flux distribution is the largest. With the decrease of the angle between the molecular axis and the z-axis, the oscillation in the electron flux distribution becomes weakened. As $\theta_D=0$, which is the case of the molecular axis direction parallel to the z-polarized laser light [17], the oscillation in the electron flux distribution is the smallest. From this figure, we also find at the given point (x=0,y=0,z=L) in the observation plane, the electron flux is the largest at $\theta_D=\pi/2$ and the smallest at $\theta_D=0$. The reasons are as follows: from Eq. (17), we find as x=0, y=0, z=L, the electron flux can be described as follows:

$$j_z(r,\theta,\varphi)=\frac{k|C|^2}{L^2}(1+\cos(kd\cos\theta_D)]. \tag{18}$$

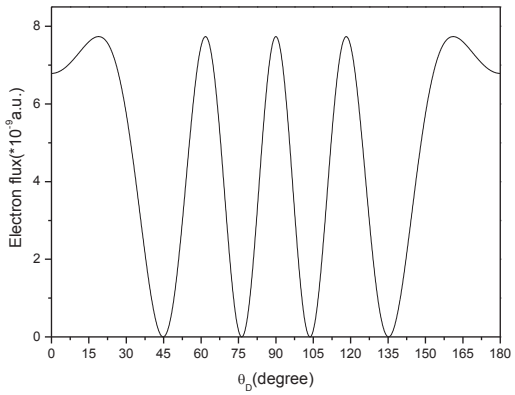

Figure 3: The electron flux distribution versus θ_D for the photodetachment of H_2^- with different molecular orientation at a given point (x=0, y=0, z=L) in the observation plane. The distance between the two centers of the H_2^- is d=4.0a.u.. The photon energy is $E_{ph}=150eV$.

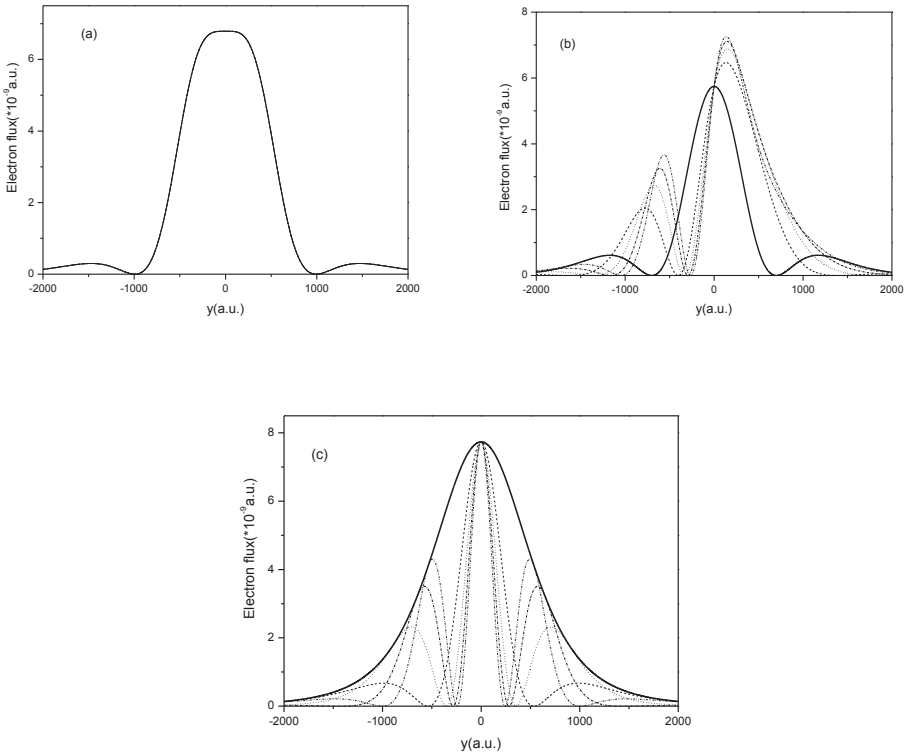

Figure 4: The variation of the electron flux distribution for the photodetachment of H_2^- with different θ_D. (a) $\theta_D = 0$,(b) $\theta_D = \pi/6$,(c) $\theta_D = \pi/2$. The solid line is $\varphi_D = 0$, the dashed line is $\varphi_D = \pi/6$, the dotted line is $\varphi_D = \pi/4$, the dash-dotted line is $\varphi_D = \pi/3$ and the dash-dotted-dotted line is $\varphi_D = \pi/2$.

The electron flux at this given point is only related to θ_D.

In Fig. 3, we plot the electron flux at this point versus θ_D. From this figure, we find at $\theta_D = \pi/3$, $\theta_D = \pi/2$, the electron flux attains maximum and the interference is totally constructive. However, at $\theta_D = \pi/4$, the electron flux attains minimum and the interference is totally destructive.

In Fig. 4, we fix the angle θ_D and discuss the influence of the value of φ_D on the electron flux distribution. Fig. 4(a) is the case with $\theta_D = 0$, and the value of φ_D is varied between 0 to $\pi/2$. We find that the electron flux distribution does not change with φ_D. The reason can be interpreted as follows: As $\theta_D = 0$, the electron flux distribution approaches the case of the molecular axis parallel to the z-polarized laser light, which is given by Eq. (11) and has no relation with the angle φ_D. Fig. 4(b) is the case with $\theta_D = \pi/6$. This plot suggest at $\varphi_D = 0$, the oscillation amplitude is the smallest. With the increase of the value φ_D, the oscillation becomes strengthened. At $\varphi_D = \pi/2$, the oscillation amplitude is the largest. Fig. 4(c) is the case with $\theta_D = \pi/2$. Under this condition, the molecular axis lies in the x-y plane, which is perpendicular to the z-polarized laser light. We find as $\varphi_D = 0$, there is only one peak in the electron flux distribution. With the increase of the value φ_D, the oscillation peaks becomes increased.

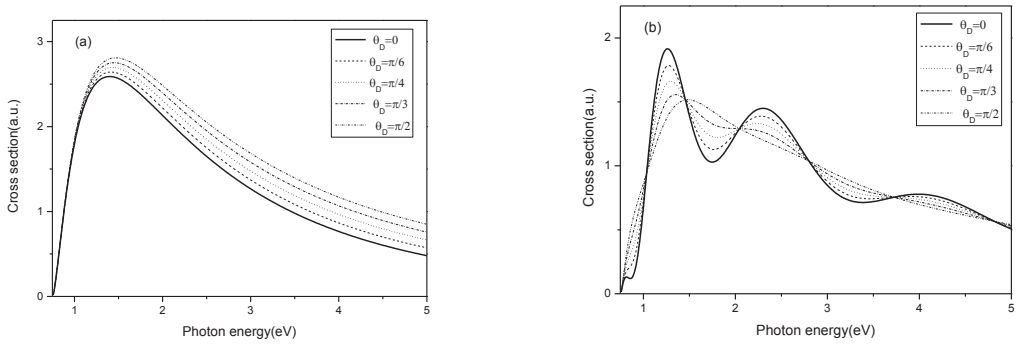

Figure 5: The photodetachment cross section of H_2^- with different molecular orientation and different distance between the two centers. (a) d=4.0a.u., $\varphi_D=\pi/6$; (b) d=40.0a.u., $\varphi_D=\pi/6$. The angle between the molecular axis and the z-axis in each plot is as follows: $\theta_D=0$ (solid line), $\theta_D=\pi/6$ (dashed line), $\theta_D=\pi/4$ (dotted line), $\theta_D=\pi/3$ (dash dotted line), $\theta_D=\pi/2$ (dash dot dotted line).

Finally, we discuss the influence of the molecular orientation on the photodetachment cross section of H_2^-. The results are given in Fig. 5. Fig. 5(a) is the result with the distance between the two centers is very small, d=4.0a.u.. In this plot, we fix the angle $\varphi_D=\pi/6$ and θ_D is varied between 0 and $\pi/2$. For different molecular orientation, the structure of the cross sections likes the case of the photodetachment cross section of H^- without external fields, which is a smooth oscillating curve. The results also suggest at low photon energy, the cross section changes little with the variation of the molecular orientation. But at high photon energy, the difference between the cross sections begins to enlarge. The value of the cross section is the smallest with the molecular orientation pointing along the z-axis ($\theta_D=0$), while its value is the largest for the molecular axis orientation perpendicular to the z-axis ($\theta_D=\pi/2$). Fig. 5(b) is the case with the distance between the two centers is very large, d=40.0a.u.. Under this circumstance, the cross sections begin to oscillate except the case with the molecular orientation perpendicular to the z-axis ($\theta_D=\pi/2$). The results also suggest with the decrease of the angle between the molecular axis and the z-axis, the oscillation amplitude in the cross section becomes increased. As $\theta_D=0$, the total cross section equals the case of the molecular axis direction parallel to the z-polarized laser light [17], the oscillation amplitude in the cross section is the largest.

4 Conclusions

In conclusion, we have investigated the influence of the molecular orientation on the electron flux distribution and the photodetachment cross section of the diatomic molecular anion. An analytical formula for the electron flux distribution has been deduced. The results show that the molecular orientation has important effect on the electron flux distribution and the cross section. At certain molecular orientation, the interference in the electron flux distribution is totally constructive; while at some other orientations, the

interference is destructive. In general, for the molecular orientation perpendicular to the laser polarization, the interference effect in the electron flux distribution is the strongest. Presently, no experiments on the photodetachment of H_2^- have been carried out. Our studies suggest that we can control the photodetachment of diatomic molecule negative ion by changing its molecular orientation. We hope that our results will guide future experiment research on the molecular photodetachment microscope.

Acknowledgments. The author acknowledges the support of the National Natural Science Foundation of China under Grant Nos.11374133 and 11074104, and the University Science & Technology Planning Program of Shandong Province under Grant No. J13LJ04.

References

[1] Bryant,H. C.; Mohagheghi, A.; J. EStewart, J. Phys.Rev.Lett. 1987, 58, 2412-2415.
[2] Rau, A. R. P.; Wong, H. Phys. Rev.A 1988, 37, 632-635.
[3] Peters, A. D.; Jaffe, C.; Delos, J. B. Phys. Rev.A 1997, 56, 331-338.
[4] Liu, Z. Y.; Wang, D. H. Phys. Rev.A 1997, 56, 2670-2676.
[5] Du, M. L. Eur.Phys.J. D. 2006, 38 ,533-537.
[6] Peng, L. Y.; Wang Q. L.; Starace, A. F. Phys. Rev.A. 2006,74, 023402(1-8).
[7] Bracher C.; Delos,J. B. Phys. Rev. Lett. 2006, 96, 100404(1-10).
[8] Yang,G.; Zheng Y.; Chi, X. J.Phys. B. 2006, 39, 1855-1860.
[9] Yang,G.; Zheng Y.; Chi, X. Phys Rev. A. 2006, 73, 043413(1-8).
[10] Lou, Z. R.; Yang, S. Q.; Li, P.; Zhou, P. W.; Han, K. L. Phys. Chem. Chem. Phys. 2014, 16, 3749-3756.
[11] Du, M. L. Phys. Rev.A 1989,40, 4983-4988.
[12] Zhao, H. J.; Du, M. L. Phys. Rev.A 2009, 79, 023408(1-8).
[13] Blondel, C.; Delsart, C.; Goldfarb, F. J. Phys. B 2001, 34, L281-285.
[14] Blondel, C.; Delsart, C.; Valli, C.; Yiou, S.; Godefroid, M. R.; Eck, S. Van. Phys. Rev. A 2001, 64, 052504 (1-8).
[15] Blondel, C.; Chaibi, W.; Delsart, C.; Drag, C.; Goldfarb, F. ; Kroger, S. Eur. Phys. J. D.2005. 33, 335-339.
[16] Afaq, A.; Du, M. L. Commun.Theor.Phys. 2006, 46, 119-126; 2008, 50, 1401-1408.
[17] Afaq, A.; Du, M. L. J.Phys.B 2009, 42, 105101(1-8).
[18] Wang, D. H.; Tang T. T.; Wang, S. S. Mol.Phys. 2010, 108, 1385-1392.
[19] Szebehely, V. Theory of orbits (New York: Academic) (1967).